Design of Horn Antenna for HAPS (High Altitude Platform Station) in 48/47 GHz Bands

Bon-Jun Ku · Do-Seob Ahn · Jong-Min Park

Satellite Communication Application Department, ETRI-Radio & Broadcasting Laboratory

E-mail:bjkoo@etri.re.kr

ABSTRACT

This paper describes design and performance test of dual-mode horn antenna for HAPS (High Altitude Platform Station) in 47.2 - 47.5 GHz and 47.9 - 48.2 GHz bands. To obtain the optimal geometry parameters of it, the conical section is represented by a stepped transition composed of a set of cylindrical waveguide sections. For each step, the corresponding generalized scattering matrix is calculated. The elements of the matrices at the open end of the horn, are calculated by the rigorous formulas of the factorization method. To verify the theoretical results, a horn breadboard was manufactured for the medium frequency of 47.7 GHz and its radiation beam patterns were measured. The calculated and theoretical results are in good agreement.

Keyword

Horn antenna; stratospheric communication system; HAPS; scattering matrix

Ⅰ. Introduction

The High Altitude Platform Station(HAPS), which is defined as a station located on an object at an altitude of 20-50km and at a specified, nominal, fixed point relative to the earth[1], is actively preparing for the operation of the next generation of communication systems worldwide[2]. The main feature of HAPS will be its ability to increase the total capacity and the coverage area by employing the multiple beams at the altitude of about 20 km. The possible antenna configuration is chosen to maximize the performance of HAPS system from appropriate system requirements including the cell size related to the maximum antenna gain, the elevation angle, and the mass and size of its payload.

Two types of horn antennas can be used principally for the HAPS in the frequency bands of 48/47 GHz: a dual-mode conical horn and a corrugated one. If two separate antennas are used to transmitter and receiver and the operating frequency band of every antenna is sufficiently narrow in the V-band, a simple dual-mode horn can be chosen to meet the requirements. The bandwidth of corrugated horn has more wide band performance than that of dual mode horn dose. Concrete parameters of horns should be carefully analyzed to clarify their availability for the integrated Transmit/Receive (T /R) antenna. Besides the additional elements in the feeder system are required to create an integrated T /R antenna. There are a lot of difficulties in realizing a high isolation between T /R channels. Therefore, the separate transmitting and receiving antennas are considered for the horns. A dual mode horn has technological advantages in manufacturing with low cost in comparison with a corrugated horn. The use of the dual-mode conical horn is considered and the radiation beam patterns are simulated in the frequency bands of 48/47 GHz.

This paper presents the analysis results for radiation beam patterns of dual-mode horn antenna for HAPS in the bands of 48/47 GHz. Preliminarily the reference antenna radiation beam pattern complies with satellite beam radiation pattern in the fixed-satellite service employing geostationary satellites for 48/47 GHz [3]. Results of computer modeling of the dual-mode characteristics and optimal geometry calculation are presented. In order to verify the theoretical results a horn breadboard was manufactured for the medium frequency of 47.7 GHz and the radiation beam patterns were measured. The calculated and theoretical results are in good agreement.

Ⅱ. Formulation

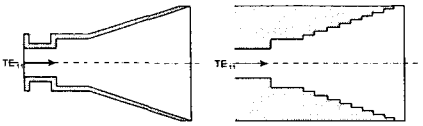

Figure 1. Horn and semi-infinite stepwise model

The horn whose characteristics corresponding to excitation by the dominant TE11 mode are required to calculate is replaced with a semi-infinite stepwise model as shown in Figure 1, and represented as a set of stacked circular waveguide sections. Thus, the key problems to be solved for it are the problems about wave scattering at a step in a circular waveguide, electromagnetic interaction between two series discontinuities, and wave radiation from an open-ended circular waveguide.

The first problem is solved by the projection mode matching. Consider a junction of two semi-infinite waveguides of radius a (Region 1) and b ($\geq a$) (Region 2). Let the junction be excited by TE and TM modes with given amplitudes A_{1n} and A_{2n} in Region 1, and given amplitudes A'_{1n} and A'_{2n} in Region 2. Then the total transverse electromagnetic field at the junction from the Regions 1 and 2 is determined by the expressions;

$$\boldsymbol{E}_{1\tau}(\rho,\varphi)=\eta\sum_{n=1}^{\infty}[(A_{1n}+B_{1n})k\sqrt{}_{1n}(a,\rho,\varphi) + (A_{2n}-B_{2n})\gamma_{2n}\ddot{\mathbf{O}}_{2n}(a,\rho,\varphi)] \quad (1)$$

$$\boldsymbol{H}_1(\rho,\varphi)\times\mathbf{e}_z=\sum_{n=1}^{\infty}[(A_{1n}-B_{1n})\gamma_{1n}\sqrt{}_{1n}(a,\rho,\varphi) + (A_{2n}+B_{2n})k\ddot{\mathbf{O}}_{2n}(a,\rho,\varphi)] \quad (2)$$

$$\boldsymbol{E}_{2\tau}(\rho,\varphi)=\eta\sum_{q=1}^{\infty}[(B'_{1q}+A'_{1q})k\ddot{\mathbf{O}}_{1q}(b,\rho,\varphi) + (B'_{2q}-A'_{2q})\gamma_{2q}\sqrt{}_{2q}(b,\rho,\varphi)] \quad (3)$$

$$\boldsymbol{H}_2(\rho,\varphi)\times\mathbf{e}_z=\sum_{q=1}^{\infty}[(B'_{1q}-A'_{1q})\gamma_{1q}\sqrt{}_{1q}(b,\rho,\varphi) + (B'_{2q}+A'_{2q})k\sqrt{}_{2q}(b,\rho,\varphi)] \quad (4)$$

where, B_{1n} and B_{2n} are unknown amplitudes of the scattered TE and TM modes in Region 1, B'_{1q} and B'_{2q} are unknown amplitudes of the scattered TE and TM modes in Region 2, η ($=120\pi$) is the wave resistance of free space,

$$\sqrt{}_{1n}(a,\rho,\varphi)=\mathbf{e}_\rho\frac{J_1(\mu_{1n}\rho/a)}{\rho N_{1n}}\sin\varphi + \mathbf{e}_\varphi\frac{\mu_{1n}J'_1(\mu_{1n}\rho/a)}{aN_{1n}}\cos\varphi \quad (5)$$

and

$$\sqrt{}_{2n}(a,\rho,\varphi)=\mathbf{e}_\rho\frac{\mu_{2n}J'_1(\mu_{2n}\rho/a)}{aN_{2n}}\sin\varphi + \mathbf{e}_\varphi\frac{J_1(\mu_{2n}\rho/a)}{\rho N_{2n}}\cos\varphi \quad (6)$$

are vector orthonormalized transverse functions of the TE and TM modes in waveguide of radius a, $J_1(...)$ and $J'_1(...)$ are the Bessel function of the first order and its derivative by argument respectively, $N_{1n}=\sqrt{\pi/2}\sqrt{\mu_{1n}^2-1}J_1(\mu_{1n})$ and $N_{2n}=\sqrt{\pi/2}\mu_{2n}J'_1(\mu_{2n})$ are normalizing coefficients, μ_{1n} and μ_{2n} are roots of the equations $J'_1(\mu)=0$ and $J_1(\mu)=0$ respectively, $\gamma_{jn}=\sqrt{k^2-(\mu_{1n}/a)^2}$ and $\gamma'_{jn}=\sqrt{k^2-(\mu_{1n}/b)^2}$ are propagation constants of the TE (j = 1) and TM (j=2) in Regions 1 and 2 respectively, $k=2\pi/\lambda$ is the wavelength, λ is the wavenumber, and $\boldsymbol{e}_\rho, \boldsymbol{e}_\varphi$, and $\boldsymbol{e}_z$ are unit vectors of the cylindrical system of coordinates ρ, φ, and z.

The projection matching of the magnetic fields (2) and (4), as well as of the electric fields (1) and (3) with taking into account the boundary condition for the field on the step, results in the system of linear algebraic equations

The generalized scattering matrix for two series discontinuities of the second problem is determined as follows. Let S_1 be the scattering matrix of the first (left) discontinuity, consisting of the blocks of reflection coefficients S_1^{11} and S_1^{22} of dimension $M_1\times M_1$ and $M\times M$ respectively, as well as of the blocks of transmission coefficients S_1^{12} and S_1^{21} of dimension $M\times M_1$ and $M_1\times M$ respectively. Similarly, let S2 be the scattering matrix of the second (right) discontinuity, consisting of the blocks of reflection coefficients S_2^{11} and S_2^{22} of dimension $M\times M$ and $M_2\times M_2$ respectively, as well as of the blocks of transmission coefficients S_2^{12} and S_2^{21} of dimension $M_2\times M$ and $M\times M_2$ respectively.

The elements of the blocks S^{11} and S^{21} of the

resulting matrix S of dimension $(M_1+M_2)\times(M_1+M_2)$ are calculated by formulas

$$S_{mn}^{11} = S_{1mn}^{11} + \sum_{q=1}^{M} S_{1mq}^{12} \exp(i\gamma_q l) B_{qn} \quad (7)$$

$$S_{mn}^{21} = \sum_{q=1}^{M} S_{2mq}^{21} \exp(i\gamma_q l) A_{qn} \quad (8)$$

where γ_q is the propagation constant of the q-th mode in the intermediate section, and l is the length of the section. The elements of the blocks S^{12} and S^{22} corresponding to the excitation of the second discontinuity from the right are determined in similar way. The elements of the scattering matrix for the open end of the circular waveguides are determined from the rigorous analytical solution obtained by Weinstein [4] with using the method of factorization.

Now, let S be the scattering matrix of the transition between the input (first) and last sections, and A_q and B_q are amplitudes of the forward and backward waves in the last section respectively, calculated as a result of solving the system for excitation of the input by the dominant TE_{11} mode. Then the reflection coefficient and radiation pattern components of the horn will be determined by formulas

$$R = S_{11}^{11} + \sum_{q=1}^{M} S_{1q}^{12} B_{q1} \exp(i\gamma_q \Delta) \quad (9)$$

$$F_{\theta/\varphi} = \sum_{q=1}^{M} A_{q1} F_{\theta/\varphi,q} \exp(i\gamma_q \Delta) \quad (10)$$

where, $F_{\theta,q}(\theta)$ and $F_{\varphi,q}(\theta)$ are the radiation patterns of the waveguide in the vertical and horizontal planes, respectively, γ_q is the propagation constant of the q-th mode in the last section, and Δ is the length of the last section.

III. Simulation and Measurement

The approach consisting in representation of the conical section as a multistep transition composed of cylindrical waveguide sections was chosen. The horn must provide axially symmetric radiation pattern of 12 ° beamwidth at 3 dB level, and gain of no less than 23 dB within two frequency bands of 47.2~47.5 GHz and 47.9~48.2 GHz. The lowest frequency of the first band and the highest frequency of the second band differ from the common central frequency of 47.7 GHz by 1.05 % respectively. Since, as known, the dual-mode horns, depending on modification, are capable to provide low level of crosspolarization in a band of up to 3~5%, it seems to be possible to provide the indicated characteristics by a single horn for both frequency bands. The calculated characteristics of such a horn are presented in Figure 2. The horn radiation patterns are calculated in the E- and H-planes for the co-polarization, and in the diagonal plane for the crosspolarization at the central frequencies of the uplink and downlink band.

The crosspolarization patterns are calculated for the angle sector where the radiation level at the co-polarization in the main beam is not lower than 20 dB. In order to verify the theoretical results, a horn breadboard for the medium frequency 47.7 GHz was manufactured and the actual radiation patterns were measured. The aim of the experimental work is to define the main horn parameters within frequency range.

The horn breadboard was made of rigid aluminum alloy by turning as shown Figure 3. A horn input is a circular waveguide of 7 mm in diameter. To have a possibility of using standard measurement equipment a waveguide transition from circular to rectangular cross-section was made.

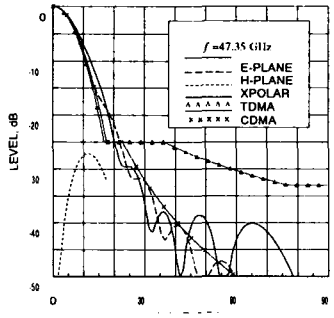

(a)

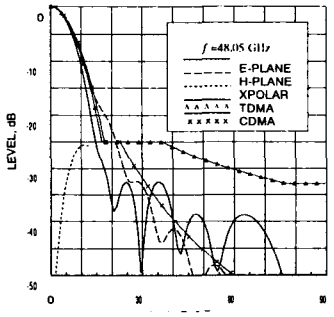

(b)

Figure 2. Radiation patterns of (a) downlink and (b) uplink

The appropriate patterns of cross-sections in E-plane and in H-plane are presented in Figure 4. The solid and dashed lines correspond to the measured and the calculated patterns respectively. We can see good agreement between the measurement and calculation results.

The shapes of main lobe and the side-lobes structure are the same even for low levels of the pattern. Some discrepancies may be considered for account of manufacturing accuracy and errors of measurements. Thus, in the calculation method used for dual-mode horn, a sufficiently accurate computer simulation should be needed to find optimal parameters of the horn in a stage of design development.

Cross-polar signal was not defined in the main pattern cross-sections because of its low level. Unfortunately, the possibilities of test equipment have not permitted to measure 45-cross-sections where the cross-polarization is of a maximum level.

IV. Conclusion

In this paper, the radiation beam pattern of dual-mode horn antenna for HAPS in the bands of 48/47 GHz were analyzed. Results of computer modeling of the dual-mode characteristics and optimal geometry calculation were presented. The calculated and measured radiation beam patterns of dual-mode horn antenna are in good agreement.

References

[1] ITU, Radio Regulations, 1 Articles, S1.66A, 1998

[2] B. J. Ku et al., "Degradation Analysis of User Terminal EIRP and G/T due to Station Keeping Variation of Stratospheric Platform, *ETRI Journal*, Vol. 22, No.1, March 2000, pp.12-19.

[3] ITU-R Rec. S.672-4, 1997.

[4] L. A. Weinstein, The Theory of Diffraction and the Factorization Method. Boulder, Colo.: Golem, 1969.

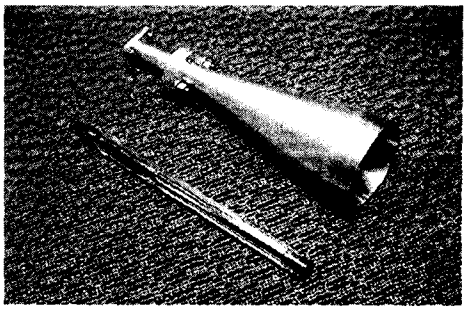

Figure 3. Manufactured dual mode horn

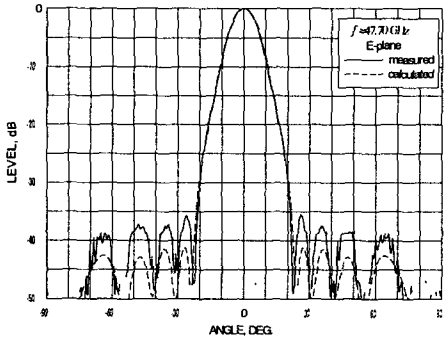

(a)

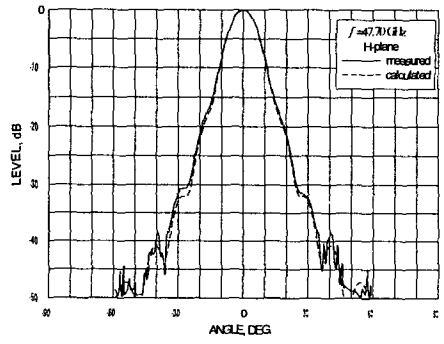

(b)

Figure 4. Pattern cross-sections of dual-mode horn at 47.7 GHz